ELSEVIER

Polymer 40 (1999) 2903–2915

polymer

Influence of particle dispersion on the matrix ligament thickness of polymer blends
2. A generalized equation and particle spatial distributions for different morphologies

Z.H. Liu[a], R.K.Y. Li[a,*], S.C. Tjong[a], C.L. Choy[b], X.G. Zhu[c], Z.N. Qi[c], F.S. Wang[c]

[a]*Department of Physics and Materials Science, City University of Hong Kong, Tat Chee Avenue, Kowloon, Hong Kong*
[b]*Department of Applied Physics, Hong Kong Polytechnic University, Hung Hom, Kowloon, Hong Kong*
[c]*State Key Laboratory of Engineering Plastics, Institute of Chemistry, Chinese Academy of Sciences, Beijing 100080, People's Republic of China*

Received 18 November 1997; revised 9 April 1998; accepted 4 July 1998

Abstract

We have derived a generalized equation for correlating the morphological parameters (matrix ligament thickness, particle spatial distribution parameter, mean particle size, particle size distribution and particle volume fraction) of polymer blends with particles obeying the log-normal size distribution. The particle spatial distribution parameters for eight regular lattices and three actual morphologies have been calculated. The particle spatial distribution parameter for the morphology of well-dispersed particles is between 1 and ca. 1.2, and is larger than those for the pseudonetwork morphology and the morphology of agglomerated particles. The relationships between the particle spatial distribution parameters defined in this work and those given in the literature are discussed.

Keywords: Polymer blends; Particle spatial distribution parameter; Morphology

Nomenclature

θ_2	∠BCG (see Fig. 1)
θ_3	∠EAB (see Fig. 1)
θ_4	Inclination angle of right-side plane to the horizontal (see Fig. 1)
0	The subscript zero denotes a regular lattice
1	The subscript one denotes the morphology of well-dispersed particles
2	The subscript two denotes the pseudonetwork morphology
3	The subscript three denotes the morphology of agglomerated particles
$l_0(1)$	Edge length of a unit cell for uniform-sized particles occupying a regular lattice
$l_0(\sigma)$	Edge length of a unit cell for particles occupying a regular lattice and obeying the log-normal distribution
l_∞	Edge length of a huge box
m	Number of particles in a unit cell
$n_\nu(1)$	Number of uniform-sized particles in a huge box
$n_\nu(\sigma)$	Number of particles in a huge box that obey the log-normal distribution
V_{cell}	Volume of a unit cell
α	Constant in Eq. (5)
L	Arithmetic average center to center interparticle distance
$L_0(1)$	Arithmetic average center to center interparticle distance for uniform-sized particles occupying a regular lattice
$L_0(\sigma)$	Arithmetic average center to center interparticle distance for particles occupying a regular lattice and obeying the log-normal distribution
L_{2D}	Arithmetic average center to center interparticle distance in 2D
L_{3D}	Arithmetic average center to center interparticle distance in 3D

* Corresponding author. Tel.: +852-27887785; Fax: +852-27887830; E-mail: aprkyl@cityu.edu.hk

0032-3861/99/$ - see front matter
PII: S0032-3861(98)00533-3

L_1 Arithmetic average center to center interparticle distance for the morphology of well-dispersed particles

L_2 Arithmetic average center to center interparticle distance for the pseudonetwork morphology

L_3 Arithmetic average center to center interparticle distance for the morphology of agglomerated particles

T Arithmetic average matrix ligament thickness (surface to surface interparticle distance)

$T_0(1)$ Arithmetic average matrix ligament thickness for uniform-sized particles occupying a regular lattice

$T_0(\sigma)$ Arithmetic average matrix ligament thickness for particles occupying a regular lattice and obeying the log-normal distribution

T_{2D} Arithmetic average matrix ligament thickness in 2D

T_{3D} Arithmetic average matrix ligament thickness in 3D

$\Delta T_{1,\xi^*}$ Error ($= T_{2D} - T_{3D}$) of T_1 arising from the reduction of dimension from 3D to 2D

d Geometric mean particle size defined by the log-normal distribution

σ Geometric mean particle size distribution parameter defined by the log-normal distribution

ϕ Particle volume fraction in the sample

ϕ_{ev} Excluded volume fraction in the sample

V Volume of particles in the sample

V_{pc} Volume of the matrix contributing to the particle cluster phase in the total sample

V_{ev} Excluded volume in the sample

ϕ_{max} Maximum particle volume fraction for uniform-sized particles

Φ_2 Volume fraction of dispersed particles in the imaginary blend with the morphology of well-dispersed particles (for the pseudonetwork morphology)

Φ_3 Volume fraction of dispersed particles in the imaginary blend with the morphology of well-dispersed particles (for the morphology of agglomerated particles)

ξ_0 Geometric constant calculated from Eq. (7) and an absolute particle spatial distribution parameter for a regular lattice

ξ_1 Relative particle spatial distribution parameter for the morphology of well-dispersed particles (the ratio of L_1 for the morphology of well-dispersed particles to L_0 for the regular lattice when d, σ and ϕ are identical)

ξ_2 Relative particle spatial distribution parameter for the pseudonetwork morphology (the ratio of L_2 for the pseudonetwork morphology to L_1 for the morphology of well-dispersed particles when d, σ and ϕ are identical)

ξ_3 Relative particle spatial distribution parameter for the morphology of agglomerated particles (the ratio of L_3 for the morphology of agglomerated particles to L_1 for the morphology of well-dispersed particles when d, σ and ϕ are identical)

ξ^* Absolute particle spatial distribution parameter for the morphology of well-dispersed particles

$\Delta\xi^*$ Error of ξ^* (calculated from Eq. (19)) defined by Eq. (25)

ξ^{**} Absolute particle spatial distribution parameter for the pseudonetwork morphology

ξ^{***} Absolute particle spatial distribution parameter for the morphology of agglomerated particles

ξ Generalized absolute particle spatial distribution parameter in Eq. (43)

δ_n Standard deviation of the particle spatial distribution parameter in small volumes or areas of a mixture defined by Eq. (45)

P Position distribution parameter defined by Eq. (46)

Φ_a Area fraction of agglomerates defined by Eq. (49)

N_{PP} Agglomeration index (the number of primary particles in the particle agglomerate) defined by Eq. (50)

1. Introduction

Many different equations for correlating the morphological parameters of spherical particle filled polymer systems have been proposed [1–18], and have been used to obtain relationships between material properties and the morphological parameters, such as that between the impact strength of polymer blends and the arithmetic average matrix ligament thickness (arithmetic average surface to surface interparticle distance) [11,12,19–26], between the impact strength of polymer blends and the arithmetic average matrix ligament thickness and particle spatial distribution parameter [16,27–29], between the toughening and stiffening efficiency and the arithmetic average matrix ligament thickness and particle spatial distribution parameter [30], between the impact strength of polymer blends and the particle position parameter [17,18,31] and between the electrical resistivity and the particle volume fraction and ratio of the radius of polymer particles to that of metal particles [1]. Clearly, different equations lead to different morphology–property relationships. Too simple an equation may neglect the important effects of some morphological parameters. For instance, the equation that relates only the arithmetic average matrix ligament thickness to the geometric mean particle size and volume fraction neglects the influences of geometric mean particle size distribution [25,26] and particle spatial distribution [16,27–29]. Recently we derived several new equations for correlating morphological parameters that are much more adequate than others for describing the relations of parameters of polymer blends with

particles obeying the log-normal size distribution. However, some improvements on these new equations are still needed.

The arithmetic average matrix ligament thickness [11,12,19–30], along with the particle dispersion parameter [16–18,27–39], are more important than other morphological parameters (average particle size, particle size distribution and particle volume fraction) in controlling the impact toughness of polymer blends and composites. The particle dispersion for the polymer blends with spherical particles conforming to the log-normal size distribution can be characterized by a particle spatial distribution parameter that is a new morphological parameter defined recently by the authors [14–16,27–30]. The morphology of well-dispersed particles and the pseudonetwork morphology are important due to their high toughening efficiency.

A new equation for correlating the morphological parameters of polymer blends with the morphology of well-dispersed particles, i.e., the arithmetic average matrix ligament thickness, the average particle size, particle size distribution and particle volume fraction, has been derived based on the simple cubic (sc) lattice assumption [13]. However, the sc lattice assumption leads to an error in the average matrix ligament thickness that can be as high as 30% [15]. Moreover, morphological observations also do not agree with this assumption. In the first paper of the present series we tried to correct the error by introducing a particle spatial distribution parameter [15]. It is interesting to note that the particle spatial distribution parameters calculated from the observed morphological parameters for several different polymer blends lie in the narrow range of 1.16 to 1.21. It is well known that direct measurements of the matrix ligament thickness from scanning electron micrographs (SEMs) may not give the true three dimensional (3D) values. Therefore, the experimental particle spatial distribution parameters obtained may not be reliable. Another problem arising from the sc lattice assumption is that the maximum particle volume fraction [39] for equal-sized particles is 0.524, so the new equation is invalid when the particle volume fraction for equal-sized particles is higher than 0.524.

It has been demonstrated that the toughening efficiency for polyvinyl chloride (PVC)/nitrile rubber (NBR) blends with the pseudonetwork morphology is much higher than that for PVC/NBR blends with the morphology of well-dispersed particles [16,27–29]. Based on the above new equation for the morphology of well-dispersed particles [13], we obtained another new equation for correlating the morphological parameters of the polymer blends with the pseudonetwork morphology [14]. Using the relationship between the impact toughness and the matrix ligament thickness and particle spatial distribution parameter, the increased toughening efficiency has been attributed to the smaller particle spatial distribution parameter for the pseudonetwork morphology [16,27–29].

It is well known that the toughening efficiency for the morphology of agglomerated particles is much lower than that for the morphology of well-dispersed particles. So, this morphology is seldom studied quantitatively. However, some new insights may be found by considering this morphology. For example, it is not known whether the morphology is adequately characterized by the particle spatial distribution parameters defined in this work and in the literature [4–10,17,18]. Consequently the relations between the morphological parameters for the morphology of agglomerated particles should be known.

In this work, we calculate the particle spatial distribution parameters for eight regular lattices and three actual morphologies. The particle spatial distribution parameters for the pseudonetwork morphology and the morphology of agglomerated particles are quantitatively related to the particle spatial distribution parameter for the morphology of well-dispersed particles. A generalized equation for correlating the morphological parameters of polymer blends or composites with spherical particles obeying the log-normal size distribution is derived. The relationships between the particle spatial distribution parameters defined by us and by other investigators are discussed.

2. A generalized equation

2.1. The regular lattice system

Fig. 1 schematically shows a unit cell for some regular arrangements. There are eight vertices (A, B, C, D, E, F, G and H), six faces and twelve edges of equal length for the unit cell. The centers of eight hard spheres are located at the eight vertices, respectively. The structural characteristics of different regular configurations are listed in Table 1.

For spheres satisfying the log-normal size distribution, the arithmetic average center to center interparticle distance L is given by [14,15]

$$L = T + d\exp\left(0.5\ln^2\sigma\right) \tag{1}$$

where T is the arithmetic average matrix ligament thickness (surface to surface interparticle distance), d is the geometric mean particle size, σ is the geometric mean particle size

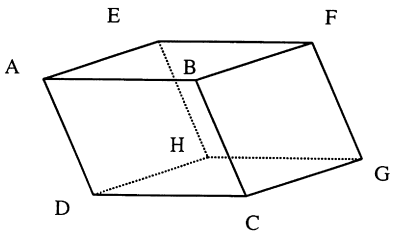

$\angle BCD=\theta_1$
$\angle BCG=\theta_2$
$\angle EAB=\theta_3$
The inclined angle of right-side plane to horizontal one=θ_4

Fig. 1. A unit cell for a regular lattice.

Table 1
Particle spatial distribution parameters for some morphologies

Morphology	θ_1	θ_2	θ_3	θ_4	m	ϕ_{max}	α[a]	ξ_0	ξ^*
sc	90°	90°	90°	90°	1	0.524[d]	1	1	
							1.238	1.238	
							1.414	1.414	
							1.416	1.416	
							1.732	1.732	
Orthorhombic (square layer)[b]	60°	90°	90°	60°	1	0.605[d]	1	1.05	
Rhombohedral (square layer)[b]	60°	60°	90°	54°44′	1	0.74[d]	1	1.12	
Orthorhombic (simple-rhombic layer)[b]	90°	90°	60°	90°	1	0.605[d]	1	1.05	
Tetragonal-sphenoidal (simple-rhombic layer)[b]	60°	104°29′	60°	63°26′	1	0.699[d]	1	1.10	
Rhombohedral (simple-rhombic layer)[b]	60°	90°	60°	70°32′	1	0.74[d]	1	1.07	
bcc	90°	90°	90°	90°	2	0.68[e]	0.866	1.09	
fcc	90°	90°	90°	90°	4	0.74[e]	0.707	1.12	
rcp						0.638[e]			1.07[f]
Well-dispersed particles[c]									
A PVC/NBR blend									1.21
A PP/EVA blend									1.18
A PP/EPDM blend									1.16

[a] Only partial results are given.
[b] The angle values are taken from Ref. [40].
[c] Data from Ref. [15].
[d] The maximum particle volume fractions for uniform-sized particles are taken from Ref. [40].
[e] Data from Ref. [42].
[f] Calculated from Eq. (19) for $T = 0$ and $\sigma = 1$.

distribution parameter, and $\sigma \geq 1$. Eq. (1) is applicable to any particle spatial distribution.

For the case of equal-sized spheres occupying a regular lattice, we have

$$T_0(1) = L_0(1) - d \tag{2}$$

where the subscript zero denotes a regular lattice. $T_0(1)$ and $L_0(1)$ but not d depend on the particle spatial distribution.

The volume of a unit cell is

$$V_{cell} = l_0(1)^3 \sin\theta_2 \sin\theta_3 \sin\theta_4 \tag{3}$$

where θ_2 is ∠BCG, θ_3 is ∠EAB, θ_4 is the inclination angle of right-side plane to the horizontal and $l_0(1)$ is the edge length of the unit cell (see Fig. 1).

The particle volume fraction ϕ is thus given by

$$\phi = \frac{\pi m d^3}{6V_{cell}} \tag{4}$$

where m is the number of spheres in one cell.

For a unit cell having edges of equal length, we have

$$L_0(1) = \alpha l_0(1) \tag{5}$$

where α is a constant which is dependent on the $L_0(1)$ considered.

Combination of Eqs. (3)–(5) gives

$$L_0(1) = \alpha\left(\frac{m}{\sin\theta_2 \sin\theta_3 \sin\theta_4}\right)^{\frac{1}{3}} d\left(\frac{\pi}{6\phi}\right)^{\frac{1}{3}}. \tag{6}$$

Let

$$\xi_0 = \alpha\left(\frac{m}{\sin\theta_2 \sin\theta_3 \sin\theta_4}\right)^{\frac{1}{3}}. \tag{7}$$

From Eqs. (2), (6) and (7), we obtain

$$T_0(1) = d\left[\xi_0\left(\frac{\pi}{6\phi}\right)^{\frac{1}{3}} - 1\right]. \tag{8}$$

Eq. (7) indicates that ξ_0 is a geometric constant. Moreover, Eq. (8) suggests that ξ_0 depends on the particle dispersion and is thus a particle spatial distribution parameter. Eq. (8) is also applicable to the body-centered cubic (bcc) or face-centered cubic (fcc) lattices though their unit cells are different from that presented in Fig. 1.

The values of ξ_0 for 8 different regular arrangements corresponding to some values of α are listed in Table 1. It should be noted that $L_0(1)$ is not necessarily equal to $l_0(1)$. For instance, there are at least three different values (corresponding to the line segments AD, AC and AG) of $L_0(1)$ in the case of particles occupying a sc lattice. For a sc lattice $\xi_0 = 1$, 1.414 and 1.732 for $\alpha = 1$ ($L_0(1)$ = the length of line segment AD), $\alpha = 1.414$ ($L_0(1)$ = the length of line segment AC) and $\alpha = 1.732$ ($L_0(1)$ = the length of line segment AG), respectively. The coordination number of a sc lattice is 6. In other words, the number of nearest particles for this lattice is 6, $\alpha = 1$, and $\xi_0 = 1$. If the 12 second nearest particles are also considered, the total nearest particle number is $6 + 12 = 18$, and the corresponding average values of α and ξ_0 are $[l_0(1) \times (6 + 12 \times 1.414)/18]/l_0(1) = 1.238$ and 1.238. If the 8 third nearest particles are also considered, the total nearest particle number is $6 + 12 + 8 = 26$, and the corresponding average values of α and ξ_0 are $[l_0(1) \times (6 + 12 \times 1.414 + 8 \times 1.732)/26]/l_0(1) = 1.416$ and 1.416. Therefore ξ_0 depends on α, as predicted by Eq. (7), and both of them

depend on the nearest particle number used in the evaluation of average values, even for a fixed lattice type. It is clear that α and ξ_0 increase with the nearest particle number. Although the nearest particle number for a sc lattice increases quickly from 6 to 26, the increase in α and ξ_0 is rather slow (from 1 to 1.416). Some values of ξ_0 for other regular lattices are listed in Table 1. It is found that ξ_0 can be identical even if the lattices are different. For example, the ξ_0 value for both the rhombohedral lattice and the fcc lattice is 1.12.

For the polydisperse sizes of particles conforming to the log-normal distribution, the relationship between $T_0(\sigma)$ and $T_0(1)$ is [13]

$$T_0(\sigma) = \left[T_0(1) + d\right]\exp\left(1.5\ln^2\sigma\right) - \exp\left(\ln d + 0.5\ln^2\sigma\right). \tag{9}$$

Here we show that Eq. (9), which was derived by assuming that the particles occupy a sc lattice [13], is also applicable to the other regular lattices listed in Table 1. In other words, it is independent of the type of regular lattice. We assume that there is a huge box with twelve edges of equal length (The length of each edge is l_∞. So, $l_\infty/l_0(1) \gg 1$), where there are $n_\nu(1)$ equal-sized particles, and $n_\nu(1)/m$ unit cells. When d and ϕ are identical, the particle number $n_\nu(\sigma)$ for particle sizes obeying the log-normal distribution in the same box is given by [13]

$$n_\nu(\sigma) = n_\nu(1)\exp\left(-4.5\ln^2\sigma\right). \tag{10}$$

We have pointed out that Eq. (10) is applicable to any lattice. We construct another unit cell that has the same type of lattice as the above unit cell for the monodisperse size of particles but with different edge length. However, the length $l_0(\sigma)$ ($l_\infty/l_0(\sigma) \gg 1$) of each edge of the unit cell for the polydisperse sizes of particles is greater than $l_0(1)$ since $n_\nu(\sigma)$ decreases with increasing $\sigma(n_\nu(\sigma) \le n_\nu(1))$, so that all these enlarged unit cells can just fill up the huge box. So, the following relation exists

$$l_\infty = \sqrt[3]{\frac{n_\nu(1)}{m}}\,l_0(1) = \sqrt[3]{\frac{n_\nu(\sigma)}{m}}\,l_0(\sigma). \tag{11}$$

From Eqs. (10) and (11), we have

$$\frac{l_0(\sigma)}{l_0(1)} = \exp\left(1.5\ln^2\sigma\right). \tag{12}$$

The relationship of $L_0(1)$ with $l_0(1)$ is

$$L_0(\sigma) = \alpha l_0(\sigma). \tag{13}$$

Combination of Eqs. (2), (5), (12) and (13) yields

$$L_0(\sigma) = L_0(1)\exp\left(1.5\ln^2\sigma\right) = \left[T_0(1) + d\right]\exp\left(1.5\ln^2\sigma\right). \tag{14}$$

For the polydisperse sizes of particles, the sum of Eq. (1) gives

$$L_0(\sigma) = \frac{\sum_{i=1}^{N} n_i L_i}{\sum_{i=1}^{N} n_i} = \frac{\sum_{i=1}^{N} n_i T_i}{\sum_{i=1}^{N} n_i} + \frac{\sum_{i=1}^{N} n_i d_i}{\sum_{i=1}^{N} n_i} = T_0(\sigma) + \frac{\sum_{i=1}^{N} n_i d_i}{\sum_{i=1}^{N} n_i}. \tag{15}$$

Because d is identical and particle sizes obey the log-normal distribution, we have [13]

$$\frac{\sum_{i=1}^{N} n_i d_i}{\sum_{i=1}^{N} n_i} = \exp\left(\ln d + 0.5\ln^2\sigma\right). \tag{16}$$

Combining Eqs. (14)–(16) and rearranging, we also obtain Eq. (9).

Insertion of Eq. (8) into Eq. (9) yields

$$T_0(\sigma) = d\left[\xi_0\left(\frac{\pi}{6\phi}\right)^{\frac{1}{3}}\exp\left(1.5\ln^2\sigma\right) - \exp\left(0.5\ln^2\sigma\right)\right]. \tag{17}$$

Eq. (17) gives the exact relation between $T_0(\sigma)$ and d, σ, ϕ and ξ_0 for the blends with spheres occupying a regular lattice and conforming to the log-normal distribution.

2.2. The morphology of well-dispersed particles

The morphology of well-dispersed particles is schematically pictured in Fig. 2, where the dark dots denote the dispersed particles and the white area in the frame indicates the polymer matrix. This morphology may be described by the fact that the probability of finding a particle in the polymer matrix for this morphology is not zero [14].

We define the relative particle spatial distribution for the morphology of well-dispersed particles by the parameter

$$\xi_1 = \frac{L_1}{L_0} \tag{18}$$

where the subscript '1' indicates the morphology of well-dispersed particles.

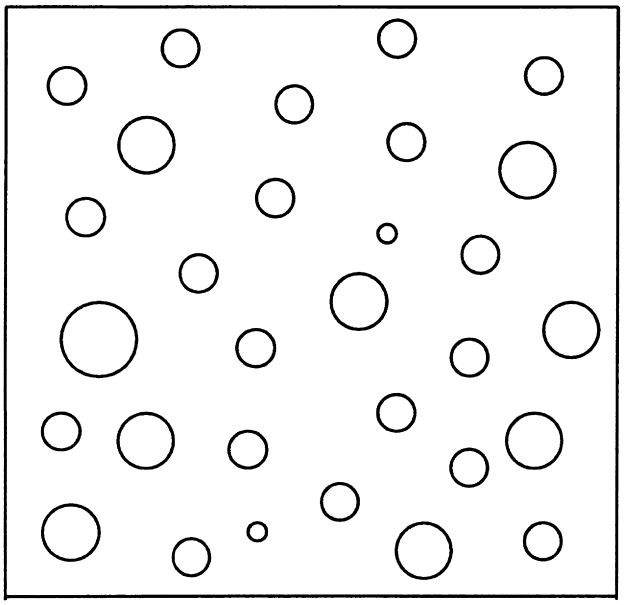

Fig. 2. The morphology of well-dispersed particles.

The relative particle spatial distribution parameter ξ_1 is the ratio of L_1 for the morphology of well-dispersed particles to L_0 for the regular lattice when d, σ and ϕ are identical. The difference between the morphology of well-dispersed particles and a regular lattice can be corrected by using ξ_1. Because Eq. (1) for evaluating L is applicable to any lattice, we can use Eq. (18) and other equations to derive Eq. (19) given below without reconstructing a unit cell in Fig. 2.

Combination of Eqs. (1), (2), (17) and (18) yields

$$T_1 = d\left[\xi^*\left(\frac{\pi}{6\phi}\right)^{\frac{1}{3}}\exp\left(1.5\ln^2\sigma\right) - \exp\left(0.5\ln^2\sigma\right)\right] \tag{19}$$

$$\xi^* = \xi_0\xi_1 \tag{20}$$

where ξ^* is the absolute particle spatial distribution parameter for the morphology of well-dispersed particles.

Combination of Eqs. (1), (17), (18) and (20) yields

$$\xi^* = \frac{T_1 + d\exp\left(0.5\ln^2\sigma\right)}{T_0(\sigma) + d\exp\left(0.5\ln^2\sigma\right)} = \frac{L_1}{d\left(\frac{\pi}{6\phi}\right)^{\frac{1}{3}}\exp\left(1.5\ln^2\sigma\right)}. \tag{21}$$

Eq. (21) shows that ξ^* is independent of the morphological parameters (α, l_0, m, θ_2, θ_3, θ_4, L_0 and ξ_0) of a regular lattice. So, the morphology of well-dispersed particles can be simulated by using any regular lattice. But, we must consider ϕ since it determines the validity of the definition of ξ_1 by Eq. (18). This point is explained as follows.

The relations between morphological parameters for the blends with the morphology of well-dispersed particles can be exactly expressed by Eq. (19). The definition of ξ_1 in Eq. (18) is generally valid for this morphology, which is different from the definition in Ref. [15] where L_0 is associated with a sc lattice for $\alpha = 1$. The failure of the earlier definition of ξ_1 can be easily seen by considering the close packing of equal-sized spheres. The maximum volume fraction ϕ_{max} for equal-sized spheres occupying a sc lattice is 0.524. So, if the earlier definition of ξ_1 is employed, Eq. (19) will be invalid when ϕ is higher than 0.524. A number of regular lattices that have higher ϕ_{max} are listed in Table 1. These lattices provide Eq. (18) with alternative ϕ_{max} for close packing of equal-sized spheres. For actual polymer blends with the morphology of well-dispersed particles, ξ^* may be approximately constant. If so, it is convenient to use Eq. (19) and other equations containing ξ^*.

Our simulations in this work show that the equation for any lattice takes the same form as Eq. (19). We know that ξ^* for the morphology of well-dispersed particles is greater than one [15]. We may obtain the maximum value of ξ^* from Eq. (19) if other parameters are measured experimentally. We have calculated the values of ξ^* for poly(vinyl chloride) (PVC)/nitrile rubber (NBR), polypropylene (PP)/EPDM and PP/EVA blends [15]. The values calculated from

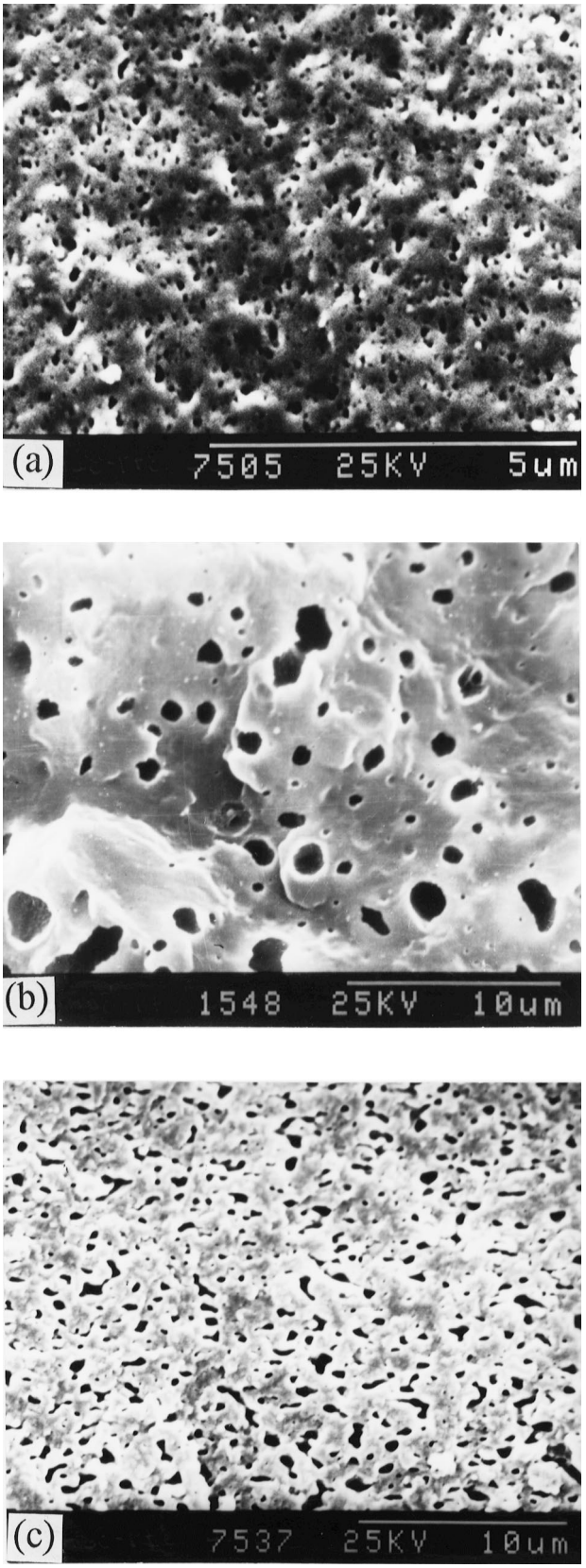

Fig. 3. SEM micrographs for (a) PVC/NBR; (b) PP/EPDM and (c) PP/EVA blends.

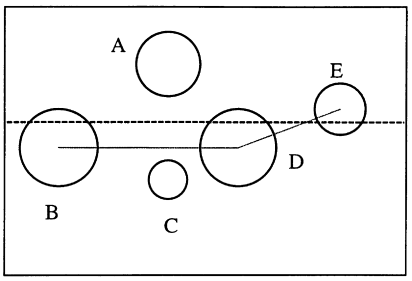

Fig. 4. Schematic illustration of the relations of center to center interparticle distance and of surface to surface interparticle distance to their real values.

Eq. (19) are 1.21, 1.18 and 1.16, indicating that the morphology of well-dispersed particles deviates from a sc lattice. Fig. 3a–3c show the SEM pictures for PVC/NBR (Fig. 3a), PP/EPDM (Fig. 3b) and PP/EVA (Fig. 3c) blends. Because the dispersed particles were removed [13], they appear dark in these pictures.

These calculated results are greater than the actual values, as will be explained below. Fig. 4 schematically illustrates the errors of the experimental values L_{2D} (arithmetic mean center to center interparticle distance in two dimensions) and T_{2D} (arithmetic mean surface to surface interparticle distance in 2D) from the real three-dimensional values, L_{3D} (arithmetic mean center to center interparticle distance in 3D) and T_{3D} (arithmetic mean surface to surface interparticle distance in 3D). Let us assume that all particle centers in this figure are located on the same plane, for instance the present paper plane. The neighbors of sphere D are spheres A, C and E. The dashed line represents the cryo-fracture surface for SEM observation or the microtomed surface for TEM observation (The two surfaces are perpendicular to the present paper plane). The spheres A and C disappear on the SEM or TEM pictures. The spheres B, D and E can be observed while the observation surface does not cut through their centers. The sphere B is not a neighbor of sphere D. Therefore the lengths of $L_{2D,BD}$ and $T_{2D,BD}$ given by the dashed line segments are longer than the dotted line segments $L_{3D,BD}$ and $T_{3D,BD}$. Although spheres D and E are neighbors, the measured dashed line segment $L_{2D,DE}$ is shorter than the dotted line segment $L_{3D,DE}$. The measured dashed line segment $T_{2D,DE}$ is longer than the dotted line segment $T_{3D,DE}$.

In general, the above analysis suggests that for any two neighboring particles

$$T_{2D,i} \geq T_{3D,i} \tag{22}$$

where the subscript $i = 1,2,...,n$. $T_{2D,i} = T_{3D,i}$ only when the observation surface cuts through two neighboring particles.

Because the observation surface does not always cut through sphere centers

$$T_{2D,j} > T_{3D,j} \tag{23}$$

where the subscript $j < i$ and is a positive integer.

Thus

$$T_{2D} = \frac{\sum_{i=1}^{N} n_i T_{2D,i}}{\sum_{i=1}^{N} n_i} > T_{3D} = \frac{\sum_{i=1}^{N} n_i T_{3D,i}}{\sum_{i=1}^{N} n_i}. \tag{24}$$

Clearly T_{2D} will be greater if a $T_{2D,k}$ (where the subscript k ($<i$) is a positive integer) for any two non-neighboring particles is included in the calculation of T_{2D}.

So, the real value of ξ^* should be evaluated from Eq. (18) where $L_1 = L_{3D}$ or from Eq. (21) where $T_1 = T_{3D}$.

However it is difficult to tell which of L_{2D} or L_{3D} is greater because some $L_{2D,i}$ s may be larger than their $L_{3D,i}$ s while some others may be smaller than their $L_{3D,i}$ s. Consequently calculating ξ_1 and ξ^* using L_{2D} may not give the real value of ξ^*.

Now we analyze the effect of the error $\Delta T_{1,\xi^*}$ (where 'Δ' denotes error) of T_1 arising from the reduction of dimension from 3D to 2D on $\Delta\xi^*$ because $\Delta\xi^*$ determines if there is an approximate constant ξ^*. $\Delta\xi^*$ is defined by

$$\Delta\xi^* = \frac{T_{2D} - T_{3D}}{d\left(\frac{\pi}{6\phi}\right)^{\frac{1}{3}} \exp\left(1.5 \ln^2\sigma\right)} = \frac{\Delta T_{1,\xi^*}}{d\left(\frac{\pi}{6\phi}\right)^{\frac{1}{3}} \exp\left(1.5 \ln^2\sigma\right)}. \tag{25}$$

For different polymer blends, $\Delta T_{1,\xi^*}$ may change dramatically. The effect of the error $\Delta T_{1,\xi^*}$ on $\Delta\xi^*$ can be more simply analyzed by the relative error $\Delta T_{1,\xi^*}/T_{2D}$. The relationship of $\Delta\xi^*$ with $\Delta T_{1,\xi^*}/T_{2D}$ is given by

$$\Delta\xi^* = \frac{T_{2D}}{d\left(\frac{\pi}{6\phi}\right)^{\frac{1}{3}} \exp\left(1.5 \ln^2\sigma\right)} \left(\frac{\Delta T_{1,\xi^*}}{T_{2D}}\right). \tag{26}$$

The effects of $\Delta T_{1,\xi^*}/T_{2D}$ in PVC/NBR, PP/EPDM and PP/EVA blends are analyzed based on Eq. (26) and the data in Table 2. Drawing scalene triangles connecting the centers of adjacent particles on SEM or TEM micrographs to measure $T_{2D,i}$ had been suggested [40] and was previously used for PVC/NBR, PP/EPDM and PP/EVA blends by the authors [13]. We think that the longer the $T_{2D,i}$ value the greater the possibility that it is actually a $T_{2D,k}$. So we measure a higher number of smaller $T_{2D,i}$ values in order to reduce the number of $T_{2D,k}$. Because an observation surface of SEM or TEM does not always cut through the centers of dispersed particles, there is also an error in d and σ from the reduction of dimension (from 3D to 2D). There have been theories dealing with this problem [41]. This error for the values of d and σ for these blends reported in Ref. [13] has been corrected. The values of T_{2D} were directly used to calculate ξ^* from Eq. (19) without any correction [15]. Using the data in Table 2 and Eq. (26), we obtain Fig. 5, showing the calculated variations of $\Delta\xi^*$ with $\Delta T_{1,\xi^*}/T_{2D}$ for PVC/NBR, PP/EPDM and PP/EVA blends. $\Delta\xi^*$ generally increases with $\Delta T_{1,\xi^*}/T_{2D}$. An error of 40% should be large enough for

Table 2
Morphological parameters for PVC/NBR, PP/EPDM and PP/EVA blends with the morphology of well-dispersed particles (data taken from Ref. [15])

Morphological parameters	Blends		
	PVC/NBR	PP/EPDM	PP/EVA
d, μm	0.073	0.51	0.32
σ	1.58	2.31	1.59
ϕ	0.136	0.243	0.243
T_{2D}, μm	0.109	1.50	0.307

$\Delta T_{1,\xi^*}/T_{2D}$. This large error can only result in a small error of ca. 0.2–0.3 for $\Delta\xi^*$. Thus, the calculated values of ξ^* for these blends are only ca. 0.2–0.3 greater than their real values. Because their real values are greater than one [15], ξ^* for the morphology of well-dispersed particles is between 1 and ca. 1.2. Moreover, we suggest that ξ^* is approximately constant for the morphology of well-dispersed particles ($\xi^* = 1.1$). Based on Fig. 5 we know that the values of $\Delta T_{1,\xi^*}/T_{2D}$ for PVC/NBR, PP/EPDM and PP/EVA are smaller than ca. 29, 25 and 37%, respectively.

Now we calculate the real ξ^* for the random close packing (rcp) system with uniform-sized particles using Eq. (19) because it is an extreme case for the morphology of well-dispersed particles. We may take $T \approx 0$ since the majority of particles are in contact, $\phi_{max} = 0.637$ (experimental value [42]) and $\sigma = 1$. Thus we have $\xi^* = 1.07$. This calculated value is indeed around 1.1 and in the range of 1 to 1.2. One may not say that $\xi^* = 1.07$ is the only possible value for the morphology of well-dispersed particles. This is because the values of $L_{3D,i}$ for the actual blends are not identical and differ from those for the rcp system where the values of $L_{3D,i}$ are very similar and 1.07 is one of the values of ξ^* for the morphology of well-dispersed particles. However, it is difficult to obtain other values of ξ^* for the morphology of well-dispersed particles. If an approximate constant ξ^* is found, one can simulate the morphology of well-dispersed particles with the regular lattice whose ξ_0 is close to the approximate constant ξ^*. In this case, $\xi_1 \approx 1$.

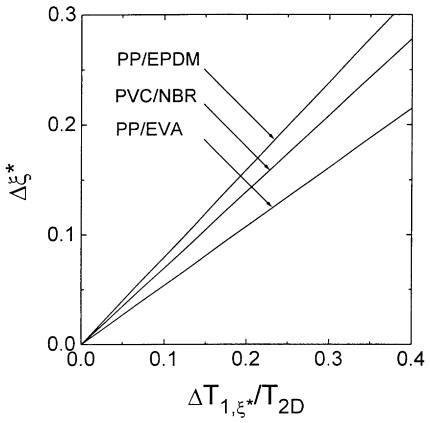

Fig. 5. Calculated variations of $\Delta\xi^*$ with $\Delta T_{1,\xi^*}/T_{2D}$ for PVC/NBR, PP/EPDM and PP/EVA blends.

Based on this criterion one can use one regular lattice in Table 1.

It must be pointed out that ξ^* is proportional to L_1 when other parameters in Eq. (21) are identical. It is clear that L_1 increases with the nearest particle number for averaging L_1. So does ξ^*. Other theoretical simulations are required to find out the dependence of ξ^* on the nearest particle number for averaging L_1. If an approximate constant ξ^* that is desired to have a weak dependence on d, σ and ϕ exists, the corresponding nearest particle number for averaging L_1 rather than other nearest particle numbers would be interesting. For actual polymer blends, we think that drawing scalene triangles connecting the centers of adjacent particles on SEM or TEM micrographs to measure $T_{2D,i}$ may have the least possibility of measuring $T_{2D,k}$ for any two non-neighboring particles compared with other experimental lattices. So, the lattice of scalene triangles is preferred. However, the corresponding nearest particle number for averaging L_1 has not been estimated because we are interested more in an approximate constant ξ^*. Experimental results of ξ^* s for the above three actual polymer blends suggest the existence of an approximate constant ξ^* regardless of the number of nearest particles.

2.3. The pseudonetwork morphology

Fig. 6 shows the pseudonetwork morphology. The pseudonetwork morphology is composed of two parts [14,16]: (1) the pseudonetwork band phase containing the particles uniformly dispersed in the band (dark dots) and the polymer matrix, and (2) the pseudonetwork core phase (dashed circles) consisting of polymer or inorganic fillers. For simplicity of drawing, we present the pseudonetwork cores as spheres. In fact, there is no shape restriction to the

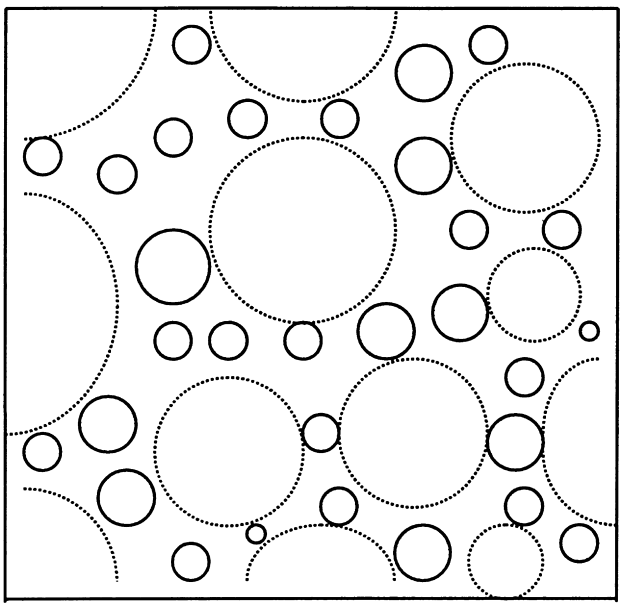

Fig. 6. The pseudonetwork morphology.

pseudonetwork cores. The probability of finding a dispersed particle (dark dots) in the pseudonetwork core phase is zero [14]. However, the probability of finding a dispersed particle in the pseudonetwork band phase must be greater than zero [14]. The pseudonetwork band phase is continuous while the pseudonetwork core phase can be continuous or discontinuous.

If the pseudonetwork band phase is regarded as a 'blend' with the morphology of well-dispersed particles [14,16], we have

$$T_2 = d\left[\xi^*\left(\frac{\pi}{6\Phi_2}\right)^{\frac{1}{3}}\exp\left(1.5\ln^2\sigma\right) - \exp\left(0.5\ln^2\sigma\right)\right] \quad (27)$$

where Φ_2 is the volume fraction of dispersed particles in the imaginary blend with the morphology of well-dispersed particles and the subscript '2' denotes pseudonetwork morphology.

The relation of Φ_2 to the volume fraction ϕ of dispersed particles in the whole sample is [14,16]

$$\Phi_2 = \frac{\phi}{\xi_2^3} \quad (28)$$

where ξ_2 is given by [14,16]

$$\xi_2 = \sqrt[3]{1-\phi_{ev}} \quad (29)$$

where ϕ_{ev} is the volume fraction of pseudonetwork cores in the whole sample. The subscript 'ev' denotes excluded volume.

Insertion of Eq. (28) into Eq. (27) yields

$$T_2 = d\left[\xi^{**}\left(\frac{\pi}{6\phi}\right)^{\frac{1}{3}}\exp\left(1.5\ln^2\sigma\right) - \exp\left(0.5\ln^2\sigma\right)\right] \quad (30)$$

$$\xi^{**} = \xi_0\xi_1\xi_2 = \xi^*\xi_2 \quad (31)$$

where ξ^{**} is the absolute particle spatial distribution parameter for the pseudonetwork morphology.

From Eqs. (1), (19) and (30), the definition of the relative particle spatial distribution parameter ξ_2 for the pseudonetwork morphology is given by

$$\xi_2 = \frac{\xi^*\xi_2 d\left(\frac{\pi}{6\phi}\right)^{\frac{1}{3}}\exp\left(1.5\ln^2\sigma\right)}{\xi^* d\left(\frac{\pi}{6\phi}\right)^{\frac{1}{3}}\exp\left(1.5\ln^2\sigma\right)} = \frac{T_2 + d\exp\left(0.5\ln^2\sigma\right)}{T_1 + d\exp\left(0.5\ln^2\sigma\right)} = \frac{L_2}{L_1}. \quad (32)$$

Therefore ξ_2 is the ratio of L_2 for the pseudonetwork morphology to L_1 for the morphology of well-dispersed particles when d, σ and ϕ are identical. Because particles in a blend with the pseudonetwork morphology are uniformly dispersed in the pseudonetwork band phase, any blend with the pseudonetwork morphology can be reconstructed into an imaginary blend with the morphology of well-dispersed particles. In other words, there is no volume restriction to reconstruction during which the pseudonetwork core phase (excluded volume) is taken away from the actual blend. So, the definition of Eq. (32) is always valid. The difference between the pseudonetwork morphology and the morphology of well-dispersed particles can be corrected by ξ_2. The difference between the pseudonetwork morphology and a regular lattice can be corrected by $\xi_1\xi_2$.

2.4. The morphology of agglomerated particles

Fig. 7 displays the morphology of agglomerated particles. This morphology consists of two main parts (see the upper part of Fig. 7): (1) the particle cluster phase (dashed circles) composed of the uniformly dispersed particles (dark dots) and material (the white part in the dashed circles), and (2) the excluded volume phase (outside the dashed circles) where the probability of finding a dispersed particle is zero. The excluded volume phase is continuous.

To correlate morphology parameters, we divide this morphology (the upper part of Fig. 7) into two phases: the particle cluster phase and the excluded volume phase (the lower part of Fig. 7). If the particle cluster phase is regarded as a 'blend' with the morphology of well-dispersed particles, we have

$$T_3 = d\left[\xi^*\left(\frac{\pi}{6\Phi_3}\right)^{\frac{1}{3}}\exp\left(1.5\ln^2\sigma\right) - \exp\left(0.5\ln^2\sigma\right)\right] \quad (33)$$

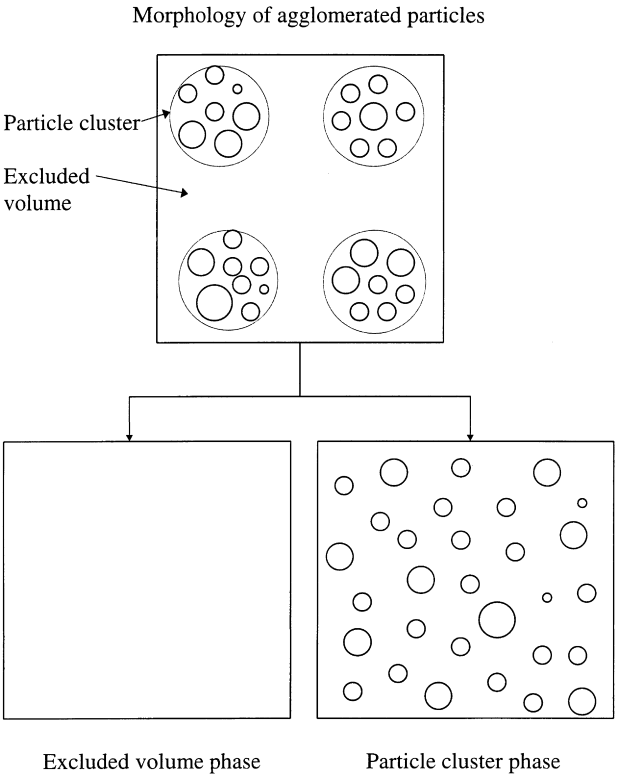

Fig. 7. The morphology of agglomerated particles.

where Φ_3 is the volume fraction of dispersed particles in the imaginary blend with the morphology of well-dispersed particles and the subscript '3' denotes morphology of agglomerated particles. Φ_3 is given by

$$\Phi_3 = \frac{V}{V + V_{pc}} \tag{34}$$

where V is the volume of particles in the entire sample, and V_{pc} is the volume of the matrix contributing to the particle cluster phase in the total sample.

The particle volume fraction ϕ is

$$\phi = \frac{V}{V + V_{pc} + V_{ev}} \tag{35}$$

where V_{ev} is the excluded volume in the total sample. The total volume of the blend is $V + V_{pc} + V_{ev}$. Therefore, ϕ is an experimental value.

The excluded volume fraction ϕ_{ev} is

$$\phi_{ev} = \frac{V_{ev}}{V + V_{pc} + V_{ev}}. \tag{36}$$

From Eqs. (34)–(36), we obtain the relation between Φ_3, ϕ and ϕ_{ev}

$$\Phi_3 = \frac{\phi}{1 - \phi_{ev}}. \tag{37}$$

Let ξ_3 be defined by

$$\xi_3 = \sqrt[3]{1 - \phi_{ev}}. \tag{38}$$

Thus

$$\Phi_3 = \frac{\phi}{\xi_3^3}. \tag{39}$$

Insertion of Eq. (39) into Eq. (33) yields

$$T_3 = d\left[\xi^{***}\left(\frac{\pi}{6\phi}\right)^{\frac{1}{3}}\exp\left(1.5\ln^2\sigma\right) - \exp\left(0.5\ln^2\sigma\right)\right] \tag{40}$$

where ξ^{***} is given by

$$\xi^{***} = \xi_0\xi_1\xi_3 = \xi^*\xi_3. \tag{41}$$

From Eqs. (1), (19) and (40), we obtain the definition of relative particle spatial distribution parameter ξ_3 for the morphology of agglomerated particles

$$\xi_3 = \frac{\xi^*\xi_3 d\left(\frac{\pi}{6\phi}\right)^{\frac{1}{3}}\exp\left(1.5\ln^2\sigma\right)}{\xi^* d\left(\frac{\pi}{6\phi}\right)^{\frac{1}{3}}\exp\left(1.5\ln^2\sigma\right)} = \frac{T_3 + d\exp\left(0.5\ln^2\sigma\right)}{T_1 + d\exp\left(0.5\ln^2\sigma\right)} = \frac{L_3}{L_1}. \tag{42}$$

Eq. (42) shows that ξ_3 is the ratio of L_3 for the morphology of agglomerated particles to L_1 for the morphology of well-dispersed particles when d, σ and ϕ are identical. Particles in a blend with the morphology of well-dispersed particles are uniformly distributed in the particle cluster phase, any blend with the morphology of agglomerated particles can be reconstructed into an imaginary blend with the morphology of well-dispersed particles. This means that there is no volume restriction to reconstruction during which V_{ev} is taken away from the actual blend. So, the definition of Eq. (42) is always valid too. The difference between the morphology of agglomerated particles and the morphology of well-dispersed particles can be corrected by ξ_3. The difference between the morphology of agglomerated particles and a regular lattice can be corrected by $\xi_1\xi_3$.

Comparing Eqs. (17), (19), (30) and (40) with each other, we obtain a generalized equation for correlating morphological parameters

$$T = d\left[\xi\left(\frac{\pi}{6\phi}\right)^{\frac{1}{3}}\exp\left(1.5\ln^2\sigma\right) - \exp\left(0.5\ln^2\sigma\right)\right] \tag{43}$$

where ξ is given by

$$\xi = \begin{cases} \xi_0 & \text{for a regular lattice} \\ \xi^* & \text{for the morphology of well-dispersed particles} \\ \xi^{**} & \text{for the pseudonetwork morphology} \\ \xi^{***} & \text{for the morphology of agglomerated particles.} \end{cases} \tag{44}$$

3. Particle dispersion vs morphology

Eq. (17) is exact for a regular lattice. However, none of the actual morphologies, i.e., the morphology of well-dispersed particles, the pseudonetwork morphology and the morphology of agglomerated particles, is a regular lattice. Additionally, the particle spatial distribution parameter ξ_0 for a regular lattice depends on α in Eq. (5), which is a function of L_0 depending on the nearest particles for averaging. So, it is clear that simulating an actual morphology using a regular lattice will cause an error. This error can be corrected using a particle spatial distribution parameter.

The particle spatial distribution parameter ξ^* for the morphology of well-dispersed particles is greater than those for the pseudonetwork morphology ($\xi^{**} = \xi^*\xi_2$) and the morphology of agglomerated particles ($\xi^{***} = \xi^*\xi_3$) since both ξ_2 and ξ_3 are smaller than one. Nevertheless, one cannot distinguish the pseudonetwork morphology from the morphology of agglomerated particles by the particle spatial distribution parameters defined in this work because they are calculated using equations in the same form (comparing (1): Eq. (29) with Eq. (38) and (2): Eq. (31) with Eq. (41), respectively). It is also noted that a difference between the two morphologies still exists. The morphological descriptions on the three morphologies

reveal that the phase continuities are different. A new morphological parameter for characterizing the phase continuity as well as the particle spatial distribution parameter may be required for characterizing the type of morphology. The phase continuity clearly affects the properties of multiphase materials, e.g., the toughness of polymer blends and the electrical resistivity of polymers blended with conductive polymers or fillers. The pseudonetwork morphology is the most favorable morphology for toughening [26–39] or conducting [1] among the above actual morphologies. Conversely, a blend with the morphology of agglomerated particles is brittle or insulating. An intermediate behavior can be found in blends with the morphology of well-dispersed particles. However, the difference of the pseudonetwork morphology and the morphology of agglomerated particles from the morphology of well-dispersed particles decreases with reducing ϕ_{ev}. So, two parameters, the particle spatial distribution parameter and a parameter for characterizing phase continuity, are required to describe the type of morphology. But it is difficult to incorporate the two parameters into one simple equation, e.g., Eq. (43).

We now present some other models in the literature that had been used to describe the spatial distribution, regardless of a common imperfection of the first two models that the spatial distribution parameter depends on the construction of an arbitrary lattice grid. Gurland [4] suggested a quantitative measure of the degree of homogeneity of particle placement in the matrix as the standard deviation (δ_n) of the particle spatial distribution parameter in small volumes or areas of the mixture

$$\delta_n = \sqrt{\frac{1}{N}\sum_{i=1}^{N}(n_i - n)^2} \tag{45}$$

where N is the number of samples, n_i is the observed number of particles per unit volume in the ith sample and n is the arithmetic mean number of particles in N samples.

Obviously Eq. (45) predicts $\delta_n \geq 0$. For the morphology of well-dispersed particles, δ_n is close to but not necessarily equal to 0 since the change in the spatial dispersion is gradual and not abrupt. For non-uniform dispersion δ_n is greater than zero. There is an excluded volume for a blend with the pseudonetwork morphology or the morphology of agglomerated particles, indicating that particles in the blend are not uniformly dispersed. So, the values of δ_n for the two morphologies are greater than zero. Moreover, one cannot distinguish the pseudonetwork morphology from the morphology of agglomerated particles by the δ_n that is greater than zero. So, the difference between the two morphologies cannot be predicted by Eq. (45). Jang and Chang [9] have proposed modifications to Eq. (45), but the above mentioned problems have not yet been solved.

Tanaka and coworkers [5–7,18] proposed a position distribution parameter P for characterizing spatial distribution:

$$P = \frac{\sum_{i=1}^{M} p_i \ln p_i}{\ln\left(\frac{1}{M}\right)} \tag{46}$$

$$p_i = \frac{b_i}{\sum_{i=1}^{M} b_i} \tag{47}$$

where M is the total number of grids and b_i the particle area in the ith grid.

P approaches unity when the particles are uniformly dispersed, for instance in a blend with the morphology of well-dispersed particles. For non-uniform dispersion, i.e., the pseudonetwork morphology and the morphology of agglomerated particles, P is smaller than unity. However, if a blend has a P value that is smaller than unity, it is not possible to tell whether it has the pseudonetwork morphology or the morphology of agglomerated particles.

The dispersion index defined by Suetsugu [8] is

$$\textit{Dispersion index} = 1 - \Phi_a \tag{48}$$

where Φ_a is an area fraction of agglomerates defined by

$$\Phi_a = \frac{\pi}{4A\phi}\sum_{i=1}^{N} n_i D_i^2 \tag{49}$$

where A is the area under observation, ϕ the particle volume fraction, D_i the diameter of an agglomerate and n_i the number of agglomerates.

It was suggested that the dispersion index ranges between 0 for the worst case of dispersion and 1 for the best dispersion [8]. The Φ_a for the best dispersion equals 0 since all the particles are well separated and there is no agglomerate ($D_i = 0$). Thus the dispersion index for the best dispersion is 1. The values of dispersion index for the morphology of well-dispersed particles, the pseudonetwork morphology and the morphology of agglomerated particles are equal to 1 because all the particles in a blend with one of these three morphologies are well separated and there is no agglomerate ($D_i = 0$ and $\Phi_a = 0$). So, the three morphologies cannot be distinguished by the dispersion index.

Chang and Nemeth [10] also gave a description of particle dispersion by

$$N_{PP} = \frac{V_{ag}}{V_{PP}} \cong \frac{D_{w,ag}^3}{D_{w,PP}^3} \tag{50}$$

where N_{PP} is called the agglomeration index and is the number of primary particles in the particle agglomerate, V_{ag} is the volume of agglomerated particles, V_{PP} is the volume of primary particles, $D_{w,ag}$ is the weight-average particle diameter for particles in the particle agglomerate and $D_{w,PP}$ is the weight-average particle diameter for primary particles.

$N_{pp} \geq 1$ according to its definition. The smaller the N_{pp}, the better the dispersion. In general, the values of N_{pp} for the pseudonetwork morphology, the morphology of well-dispersed particles and the morphology of agglomerated particles are equal to one because particles in a blend with one of these morphologies are well separated ($D_{w,ag} = D_{w,pp}$). So, the three types of morphologies cannot be distinguished by N_{pp}.

4. Conclusions

The values of the particle spatial distribution parameter for 8 regular lattices have been evaluated. For a given lattice the particle spatial distribution parameter have several values. It is also possible that the particle spatial distribution parameter for a regular lattice is the same as that for another regular lattice. So, the particle spatial distribution parameter is not a unique parameter for determining the dispersion state of particles occupying a regular lattice.

Definitions for the particle spatial distribution parameter of three different actual morphologies, the morphology of well-dispersed particles, the pseudonetwork morphology and the morphology of agglomerated particles, have been proposed. For the morphology of well-dispersed particles, particles are uniformly dispersed in the polymer matrix, so the probability of finding a particle in the polymer matrix is not zero. There are excluded volumes in the latter two morphologies and the probabilities of finding a particle in the excluded volumes are zero. Particles in the pseudonetwork band phase are also uniformly dispersed; the pseudonetwork band phase is continuous while the pseudonetwork core phase (excluded volume) can be either continuous or discontinuous. For the morphology of agglomerated particles, particles in the particle cluster phase are uniformly dispersed; the particle cluster phase is discontinuous while the excluded volume is continuous. The latter two morphologies will transform into the morphology of well-dispersed particles when the excluded volume fraction is zero. We have emphasized the importance of a morphological parameter for characterizing the phase continuity but have not been able to give a definition.

The relationship between the experimental value (2D) of average matrix ligament thickness and the real one (3D) for the morphology of well-dispersed particles has been qualitatively analyzed. It has been proved that the former are larger than the latter. For the morphology of well-dispersed particles, the absolute particle spatial distribution parameter is proportional to the center to center interparticle distance when the other parameters in Eq. (21) are identical. Drawing scalene triangles connecting the centers of adjacent particles on SEM or TEM micrographs to measure average matrix ligament thickness had been suggested [41] and was used for PVC/NBR, PP/EPDM and PP/EVA blends by the authors [13]. The calculated values of the absolute particle spatial distribution parameter for PVC/NBR, PP/EPDM and PP/EVA blends with the morphology of well-dispersed particles are 1.21, 1.18 and 1.16, respectively [15]. Therefore the highest value for the absolute particle spatial distribution parameter of actual blends with well-dispersed particles is about 1.2. We have shown that the absolute particle spatial distribution parameter for the morphology of well-dispersed particles must be greater than one [15]. Therefore, the absolute particle spatial distribution parameter for the morphology of well-dispersed particles lies between 1 and ca. 1.2. The absolute particle spatial distribution parameter for the random close packing system (an extreme case of the morphology of well-dispersed particles) with uniform-sized particles is 1.07. We have shown that even a large error in the arithmetic average matrix ligament thickness leads to a small change (at most ca. 0.2–0.3) in the absolute particle spatial distribution parameter for the morphology of well-dispersed particles. So, we suggest that the absolute particle spatial distribution parameter for the blends with the morphology of well-dispersed particles may be roughly constant ($\sim$1.1).

We have derived a generalized equation (Eq. (43)) for relating the arithmetic average matrix ligament thickness (average surface to surface interparticle distance) to the average particle size, particle size distribution, particle volume fraction and particle spatial distribution parameter for polymer blends or composites with spherical particles obeying to the log-normal size distribution. The particle spatial distribution parameters for a regular lattice and three actual morphologies have been correlated. The absolute particle spatial distribution parameter for the morphology of well-dispersed particles is greater than those for the pseudonetwork morphology and the morphology of agglomerated particles. However, one cannot distinguish the pseudonetwork morphology from the morphology of agglomerated particles by the particle spatial distribution parameter defined in this work.

It has also been shown that the above three actual morphologies cannot be well distinguished using the parameters previously defined in the literature.

Acknowledgements

This work was financially supported largely by a City University of Hong Kong Strategic Grant (No. 700649) and partially by the Hong Kong Research Grants Council and the NSFC (China) through Grant No. 59233060.

References

[1] Malliaris A, Turner DT. J Appl Phys 1971;42:614.
[2] Lange FF, Radford KC. J Mater Sci 1971;6:1197.
[3] Dijkstra K, Ten Bolscher GH. J Mater Sci 1994;29:4286.
[4] Gurland J. In: DeHoff RT, Rhines FN, editors. Quantitative microscopy. New York: McGraw-Hill, 1968.

[5] Tanaka H, Hayashi T, Nishi T. J Appl Phys 1986;59:653.
[6] Tanaka H, Hayashi T, Nishi T. J Appl Phys 1986;59:3627.
[7] Tanaka H, Hayashi T, Nishi T. J Appl Phys 1986;59:4480.
[8] Suetsugu Y. Intern Polym Proc 1990;3:184.
[9] Jang BZ, Chang YS. In: Provder T, editor. ACS Symposium Series 332. Washington, DC: American Chemical Society, 1987:30.
[10] Chang MCO, Nemeth RL. J Appl Polym Sci 1996;61:1003.
[11] Wu S. Polymer 1985;26:1855.
[12] Wu S. J Appl Polym Sci 1988;35:549.
[13] Liu ZH, Zhang XD, Zhu XG, Qi ZN, Wang FS. Polymer 1997;38:5267.
[14] Liu ZH, Zhu XG, Zhang XD, Qi ZN, Choy CL Wang FS. Acta Polymerica Sinica 1998;1:1.
[15] Liu ZH, Li RKY, Tjong SC, Qi ZN, Wang FS, Choy CL. Polymer 1998;39:4433.
[16] Liu ZH, Zhang XD, Zhu XG, Li RKY, Qi ZN, Wang FS, Choy CL. Polymer, in press.
[17] Hayashi T, Nishi T. Kobunshi 1991;40:458.
[18] Hayashi T, Watanabe A, Tanaka H, Nishi T. Kobunshi Ronbunshu 1992;49:373.
[19] Wu S. Polym Eng Sci 1990;30:753.
[20] Jancar J, DiAnselmo A, DiBenedetto AT. Polym Commun 1991;32:367.
[21] Wu X, Zhu X, Qi Z. In: Proceedings of the 8th International Conference on Deformation, Yield and Fracture of Polymers. London, 1991:78/1.
[22] Liu CX. MS thesis, Chengdu University of Science and Technology, Chengdu, 1992.
[23] Fu Q, Wang GH, Shen JS. J Appl Polym Sci 1993;49:673.
[24] Gloaguen JM, Steer P, Gailland P, Wrotecki C, Lefebver JM. Polym Eng Sci 1993;33:748.
[25] Liu ZH, Zhu XG, Zhang XD, Qi ZN, Choy CL, Wang FS. Acta Polymerica Sinica 1996;4:468.
[26] Liu ZH, Zhu XG, Li Q, Qi ZN, Wang FS. Polymer, in press.
[27] Liu ZH, Zhu XG, Zhang XD, Qi ZN, Choy CL, Wang FS. Acta Polymerica Sinica 1997;5:565.
[28] Liu ZH, Zhang XD, Zhu XG, Qi ZN, Wang FS, Li RKY, Choy CL. Polymer, in press.
[29] Liu ZH, Zhu XG, Zhang XD, Qi ZN, Choy CL, Wang FS. Acta Polymerica Sinica 1998;1:8.
[30] Liu ZH, Zhang XD, Zhu XG, Qi ZN, Wang FS, Li RKY, Choy CL. Polymer, in press.
[31] Kayano Y, Keskkula H, Paul DR. Polymer 1996;37:4505.
[32] Breuer H, Haaf F, Stabenow J. J Macromol Sci Phys 1977;B14:387.
[33] Haaf F, Breuer H, Stabenow J. Angew Macromol Chem (Vol. 58–59) 1977:95.
[34] Keskkula H, Kim H, Paul DR. Polym Eng Sci 1990;30:1373.
[35] Kim H, Keskkula H, Paul DR. Polymer 1990;31:869.
[36] Majumdar B, Keskkula H, Paul DR. Polymer 1994;35:3164.
[37] Majumdar B, Keskkula H, Paul DR. Polymer 1994;35:5453.
[38] Majumdar B, Keskkula H, Paul DR. Polymer 1994;35:5468.
[39] Brady AJ, Keskkula H, Paul DR. Polymer 1994;35:3665.
[40] Shinohara K. In: Fayed ME, Otten L, editors. Handbook of powder science and technology. New York: Van Nostrand Reinhold, 1984.
[41] Chan SL. In: Roulin-Moloney AC, editor. Fractography and failure mechanisms of polymers and composites. London: Elsevier Science, 1989.
[42] Zellen R. The physics of amorphous solids. New York: Wiley, 1983.